0273-2289/03/105-108/0101/$20.00

Estimation of Temperature Transients for Biomass Pretreatment in Tubular Batch Reactors and Impact on Xylan Hydrolysis Kinetics

Suzanne L. Stuhler and Charles E. Wyman*

Thayer School of Engineering, Dartmouth College, 8000 Cummings Hall, Hanover, NH 03755, E-mail: Charles.Wyman@Dartmouth.edu

Abstract

A combined heat transfer/kinetic model was developed to quantify temperature variations in small tubular batch reactors and estimate the effect of deviations from isothermal operation on the kinetics of biomass pretreatment. Assuming that heat transfer was dominated by conduction in the radial direction, a classic parabolic time-dependent partial differential equation was applied to describe the temperature in the system and dedimensionalized to provide a single solution for application to all situations. A dimensionless expression for the reaction kinetics for xylan hydrolysis was then developed, and a single parameter expressed as the dimensionless ratio of the first-order rate constant times the tube radius squared divided by the thermal diffusivity was found to control the reaction rate. Three different characterizations of the deviation between the concentration profile predicted for isothermal xylan hydrolysis and that based on the transient temperature were directly related to this dimensionless rate constant parameter for both catalyzed and uncatalyzed hydrolysis kinetics. These results were then used to project the relationship between deviations in yield from isothermal results and the tube radius and reaction time.

Index Entries: Reactor design; heat transfer; kinetics; hydrolysis; pretreatment.

Introduction

The use of small-volume tubular batch reactors to study the hydrolysis kinetics of hemicellulose is common in the literature because of the relative simplicity and ease of use of this type of reactor system. The reactors can be easily filled with the desired substrate, sealed, and submerged in a constant-

*Author to whom all correspondence and reprint requests should be addressed.

temperature oil or fluidized sand bath set at the reaction temperature. Researchers have utilized 1-in. 316 SS tubing *(1)*, 0.5-in. Hastelloy tubing *(2)*, glass tube reactors *(3,4)*, and a variety of other similar apparatus to conduct experimental studies on both acid-catalyzed and uncatalyzed (autohydrolysis) hydrolysis. A common feature of these studies is that they are typically assumed to be carried out under isothermal reaction conditions *(5)*. In other words, it is assumed that the reactor and its contents instantaneously reach reaction temperature on immersion in a constant-temperature bath, and the temperature transients that occur as the reactor is heated from ambient to reaction temperature are not considered. These temperature transients result in deviations to the predicted reaction progress using isothermal kinetics *(5)*. Some researchers have acknowledged these transients and have typically dealt with them in one of two ways: (1) design a preheating strategy to minimize the temperature transients, or (2) quantify the transients for specific reaction conditions to obtain a measure of their effect on yields.

Most studies have applied the first method. For example Chen et al. *(4)* proposed a two-bath procedure in which the reactors are placed in a bath set 50°C higher than the reaction temperature for 50 s. Jacobsen *(6)* also used a two-bath procedure in which the first bath is heated to 150% of the reaction temperature. Only two published studies have been identified in which an attempt to quantify the temperature transients is made *(5,7)*. In a study by Tillman et al. *(5)*, a quantitative guideline is presented to assess the impact of temperature and chip thickness on total xylose yield for acid hydrolysis of aspen hemicellulose, and in the work of Jacobsen and Wyman *(7)*, a comparison of xylan remaining in 0.5- and 1.0-in.-diameter batch tubes was presented.

The primary objective of the present study was to develop a comprehensive model that can be used with any given set of kinetics to estimate the deviation from isothermal operation. First a dimensionless heat transfer model was derived for the tubular reactor to describe the temperature profile as a function of tube radius and time assuming that heat transfer is dominated by conduction. This model was then coupled to a dimensionless equation to describe xylan hydrolysis, and a dimensionless rate constant was devised to combine similar systems in a single equation. From this, a quantitative measure was developed between the controlling factors for reactor design and the deviation of xylan hydrolysis from isothermal operation.

Development of the Model and Dimensionless Rate Constant

First, the heat transfer portion of the combined model was derived by applying the unsteady-state equation of energy in cylindrical coordinates for one-dimensional heat conduction *(8)*:

$$\frac{\partial T}{\partial t} = \alpha \left(\frac{\partial^2 T}{\partial r^2} + \frac{1}{r} \frac{\partial T}{\partial r} \right) \tag{1}$$

in which T is the temperature, t is the time, α is the thermal diffusivity, and r is the radial position. The thermal diffusivity, α, is given by Eq. 2:

$$\alpha = \frac{k}{\rho C_p} \tag{2}$$

in which k is the thermal conductivity, ρ is the density, and C_p is the heat capacity.

To apply Eq. 1 to a tubular batch reactor system, the reactors were assumed to be infinitely long cylinders with heat transfer by only conduction in the radial direction.

One solution of this equation could be applied to multiple applications by rewriting it in dimensionless form. To this end, three dimensionless parameters were introduced: t^*, the dimensionless time; r^*, the dimensionless radius; and T^*, the dimensionless temperature, defined as follows *(8)*:

$$t^* = \frac{\alpha t}{R^2} \tag{3}$$

$$r^* = \frac{r}{R} \tag{4}$$

$$T^* = \frac{T - T_i}{T_f - T_i} \tag{5}$$

in which T_i is the initial reactor temperature, T_f is the desired reaction temperature, and R is the reactor radius. These three equations were substituted back into Eq. 1 to obtain the dimensionless heat transfer equation:

$$\frac{\partial T^*}{\partial t^*} = \frac{\partial^2 T^*}{\partial r^{*2}} + \frac{1}{r^*}\frac{\partial T^*}{\partial r^*} \tag{6}$$

This equation was solved numerically in an Excel spreadsheet using an explicit finite-difference method with 10 radial increments across the tube radius, as presented in Fig. 1. Figure 1 shows that the tube contents near the wall heat up very rapidly while the contents near the center take much longer to reach the desired reaction temperature. Because this equation is dimensionless, its solution is applicable to any combination of tubular reactor size (radius), tube contents (thermal diffusivity), initial reactor temperature, and desired reaction temperature.

A dimensionless approach was also applied to describe xylan hydrolysis based on the following first-order model for solids decomposition:

$$\frac{dX}{dt} = -kX \tag{7}$$

in which X is the hemicellulosic xylan in solid form and k is the reaction rate constant. We then introduced the dimensionless time, t^*, as previously defined and the dimensionless xylan remaining in solid form, X^*:

$$X^* = \frac{X}{X_o} \tag{8}$$

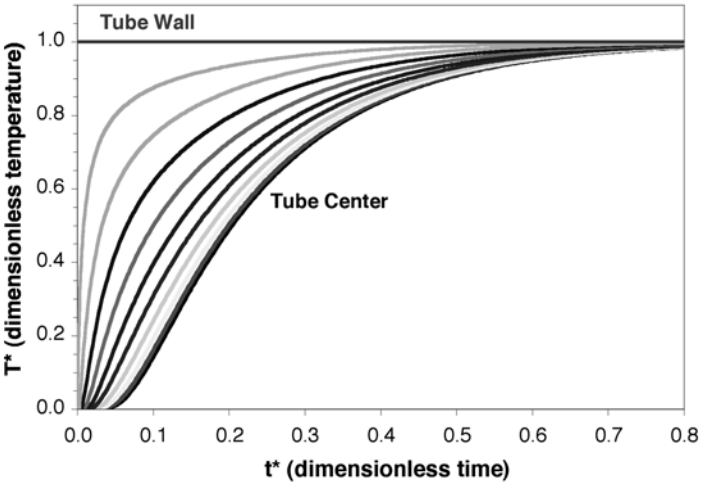

Fig. 1. Dimensionless temperature profile for tubular batch reactors showing temperature vs time for 10 radial intervals.

in which X_o is the initial amount of xylan in the substrate. Now the dimensionless kinetic expression can be written as

$$\frac{dX^*}{dt^*} = -\beta X^* \tag{9}$$

in which β, the dimensionless first-order rate constant, is

$$\beta = \left(\frac{R^2 k}{\alpha}\right) \tag{10}$$

Equation 9 can then be solved by applying the initial condition that $X^* = 1.0$ when $t^* = 0$, to obtain the following analytical expression, which describes the amount of xylan remaining in solid form as a function of dimensionless time and β only when the temperature is constant:

$$X^* = \exp\left(-\beta t^*\right) \tag{11}$$

The dimensionless rate constant, β, can be written for uncatalyzed (autohydrolysis) hydrolysis by incorporating the Arrhenius relationship for the rate constant:

$$k = k_o e^{(-E/RT)} \tag{12}$$

in which k_o is the preexponential factor, E is the activation energy, and R is the gas constant. For acid-catalyzed hydrolysis, an additional acid concentration term is added to the Arrhenius expression:

$$k = k_o C^n e^{(-E/RT)} \tag{13}$$

in which *C* is the acid concentration and *n* is the reaction order. Therefore, the dimensionless rate constants for uncatalyzed and catalyzed xylan hydrolysis, respectively, can be defined as follows:

$$\beta_{uncat} = \frac{R^2}{\alpha} k_o e^{(-E/RT)} \tag{14}$$

$$\beta_{cat} = \frac{R^2}{\alpha} k_o C^n e^{(-E/RT)} \tag{15}$$

First, the isothermal xylan profile (X^*_{iso}) was calculated as a function of dimensionless time for a given β as:

$$X^*_{iso} \equiv f\left(t^*, \beta\right) \text{ in which } \beta \equiv f\left(R, \alpha, k_o, E, T_f, C, n\right) \tag{16}$$

by applying Eq. 11 for a constant target temperature T_f in conjunction with either Eq. 14 or 15, depending on whether uncatalyzed or acid-catalyzed kinetics were being studied. Next, the above kinetic expressions given by Eqs. 9, 14, and 15 were incorporated into an Excel spreadsheet containing the transient temperature profiles presented in Fig. 1. The transient temperature xylan profile (X^*_{trans}) was calculated by dividing the batch reactor into 10 rings and calculating the relative area of the rings to determine the initial amount of xylan in each ring. Equation 11 was then integrated across each ring using Euler's method to determine the amount of xylan remaining in each ring after each time step. Instead of simply using the desired reaction temperature in this equation, the average temperature of the inner and outer radius of each radial increment was taken from the transient temperature profile and used to calculate the reaction rate constant during that increment of time. Because the actual dimensional temperature had to be used in this calculation, the transient xylan profile is dependent on the initial temperature of the reactor in addition to t^* and β:

$$X^*_{trans} \equiv f\left(t^*, \beta, T_i\right) \tag{17}$$

The two profiles were plotted and compared to produce a quantitative measure of deviation between the reaction profiles for isothermal and transient temperature as discussed in the following section. Figure 2 shows an example of a comparison of isothermal and transient profiles for a value of β = 1.0. As expected, the amount of xylan decreases more slowly for transient than for isothermal operation because of the delay in increase in temperature from the initial to target value.

Development of Quantitative Measures of Deviation from Isothermal Operation

To quantitatively describe the difference between the transient and isothermal xylan profiles, three parameters were investigated: the sum of squares of the error (SS_E), the % area difference (%*AD*), and the % instantaneous difference (%*ID*), as follows:

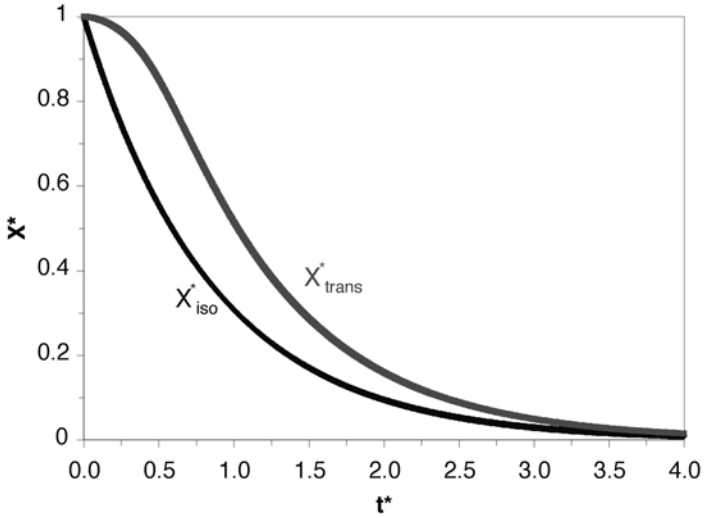

Fig. 2. Comparison of isothermal and transient reaction profiles showing dimensionless xylan remaining in solid form vs dimensionless time.

Sum of Squares of Error

SS_E was calculated by summing the squares of the differences between the predicted amounts of xylan left for transient and the amount predicted for isothermal operation over a given time span as follows:

$$SS_E = \sum_{i=0}^{n}\left(X^*_{trans}\left[t^*_o + i\Delta t^*\right] - X^*_{iso}\left[t^*_o + i\Delta t^*\right]\right)^2 \tag{18}$$

in which

$$X^*_{trans}\left(t^*_o + i\Delta t^*\right) \text{ and } X^*_{iso}\left(t^*_o + i\Delta t^*\right)$$

are, respectively, the numeric values of the predicted amounts of xylan remaining for transient and isothermal operation evaluated at a specific time. Clearly, the magnitude of this error is dependent on the number of time steps that it is evaluated over, so for the purposes of this article a constant number of time steps was used.

% Area Difference

%*AD* was based on the difference between the xylan curves for the transient and isothermal reactions divided by the integral for isothermal behavior to give a relative deviation:

$$\%AD = 100\left(\frac{\int_0^{t^*} X^*_{trans}dt^* - \int_0^{t^*} X^*_{iso}dt^*}{\int_0^{t^*} X^*_{iso}dt^*}\right) \tag{19}$$

Table 1
Experimental Conditions and Parameters for Kinetic Models

	Garrote et al. *(9)*	Chen et al. *(4)*
Pretreatment	Autohydrolysis	Dilute acid
Substrate	Corncobs	Corncob/stover mixture
Temperature range (°C)	145–190	120–150
Acid conc. range (wt%)	—	0.11–1.9
k_o	1.46×10^{12} s^{-1}	3.33×10^{8} s^{-1} $wt\%^{-1}$
E (kJ/mol)	130	86.2
n	—	1.0

% Instantaneous Difference

%*ID* was derived by subtracting the predicted amount of xylan left for isothermal operation from the predicted value for transient operation at a specified dimensionless time and dividing by the predicted quantity of xylan for isothermal reaction according to the following expression:

$$\%ID = \frac{X^*_{trans} - X^*_{iso}}{X^*_{iso}} \tag{20}$$

This parameter is different from the other two measures of deviation because it only depends on the instantaneous difference in xylan remaining and is therefore independent of the time history of the profile.

Results

To determine whether the dimensionless rate constant, β, can be correlated with a quantitative measure of deviation, the model was applied with two published kinetic models. Table 1 presents the kinetic parameters and experimental conditions that were used for the two sets.

The Excel model was run multiple times for both kinetic models by varying the reaction temperature, acid concentration (for the acid-catalyzed model), and initial temperature (20 or 100°C) within the reported range of experimental conditions. The value of β along with the three quantitative measures of deviation were calculated for each trial. Figures 3 and 4 show the deviation parameters SS_E and %*AD* defined at 100% yield (i.e., t^* at which X^*_{iso} and X^*_{trans} are equal to zero) plotted vs β for both catalyzed and uncatalyzed models for two different initial temperatures: 20 and 100°C. The scales for these figures are different for catalyzed and uncatalyzed models because the β values calculated within the experimental ranges in Table 1 are higher for the uncatalyzed model. From Figs. 3 and 4, one can see that for small values of β, there is a positive linear relationship between both deviation quantities and β. For larger values of

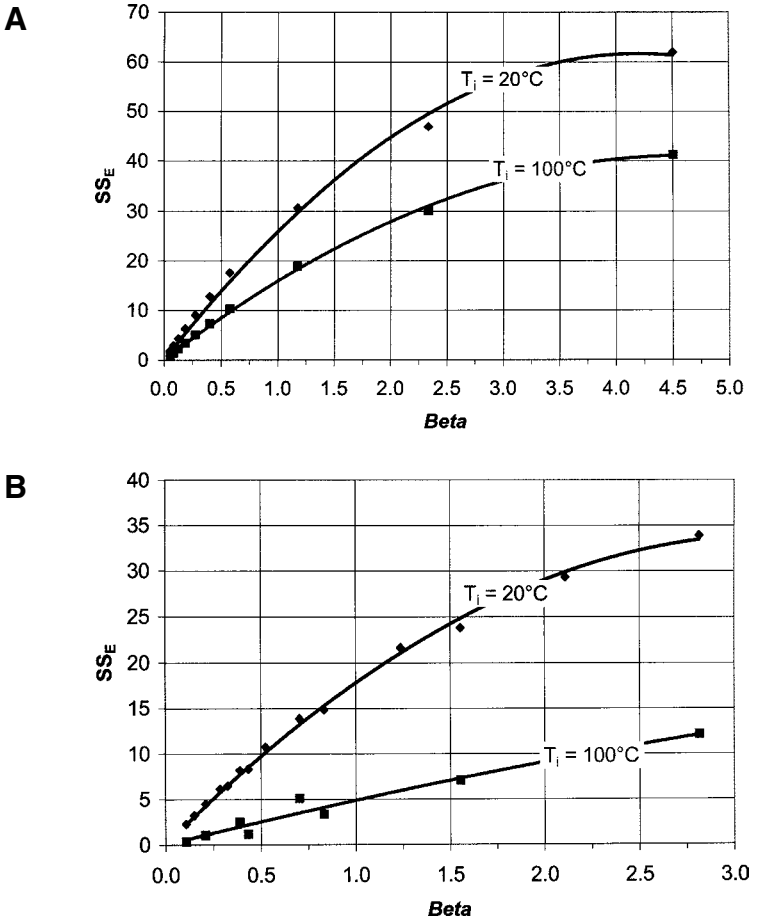

Fig. 3. SS_E vs dimensionless rate constant, β, for **(A)** uncatalyzed and **(B)** acid-catalyzed kinetic models and initial temperatures of 20 and 100°C.

β, this relationship becomes less and less linear. The linear relationship between %AD and β (Fig. 4) holds over a wider range of β than the linear relationship between the SS_E and β (Fig. 3). For both Figs. 3 and 4, a comparison of uncatalyzed plots (Figs. 3A and 4A) and catalyzed plots (Figs. 3B and 4B) shows that there is greater scatter for the catalyzed plots. This is owing to the additional parameter of acid-concentration that was included and varied in the acid-catalyzed model to obtain the data points.

The regression lines plotted in Fig. 4 for $T_i = 20$°C are very similar for the uncatalyzed and acid-catalyzed models and are given by, respectively:

$$\%AD_{uncat} = 37.5 \times \beta \tag{21}$$

$$\%AD_{cat} = 31.4 \times \beta \tag{22}$$

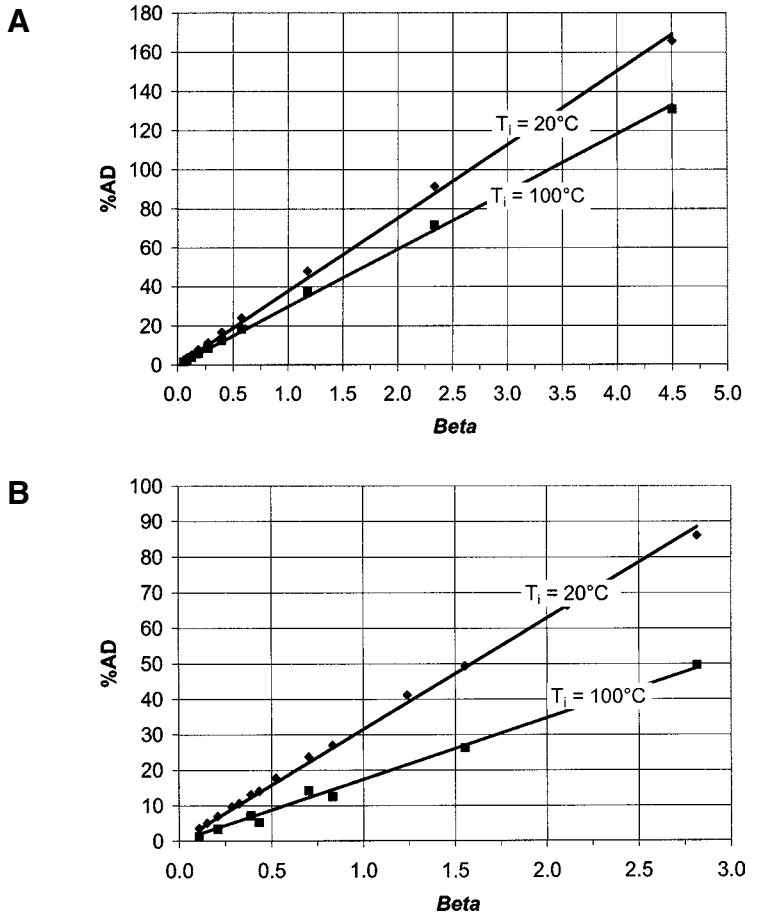

Fig. 4. %*AD* vs dimensionless rate constant, β, for **(A)** uncatalyzed and **(B)** acid-catalyzed kinetic models and initial temperatures of 20 and 100°C.

These two equations can then be used to produce a set of design curves for each kinetic model. For example, for uncatalyzed kinetics, an expression for the reaction temperature as a function of tube radius can be written at any %*AD* if the thermal diffusivity and kinetic constants are held constant. Figure 5 shows the design curves at 5, 10, 20, 50, and 100% error for both T_i = 20°C and T_i = 100°C assuming Garrote kinetics as presented in Table 1 and $\alpha = 0.0016$ cm^2/s.

A similar plot can be prepared for the acid-catalyzed kinetics using Eq. 22; however, the initial temperature and the acid concentration must be specified for each design curve. Figure 6 shows the design curves at 5, 10, 20, 50, and 100% area difference for an initial temperature of 20°C and an acid concentration of 0.5 wt%. To demonstrate the effect of varying the

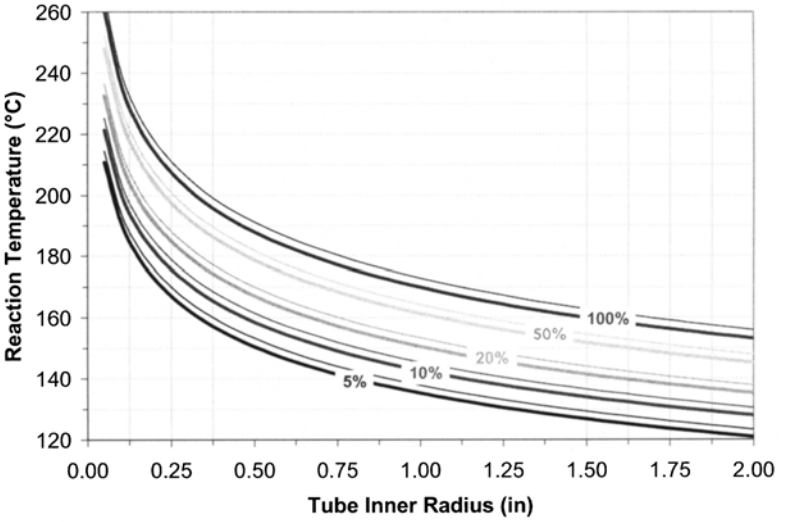

Fig. 5. %*AD* as function of tube inner radius and reaction temperature for uncatalyzed model and initial temperatures of 20°C (thick solid lines) and 100°C (thin solid lines).

acid concentration and initial temperature on the design curve for acid-catalyzed kinetics for an error of 5%, the plot in Fig. 7 was generated.

Instead of calculating the %*AD* over the entire time profile (until $X^* \rightarrow 0$) as presented in Figs. 5–7, a different plot was generated by calculating the %*AD* at a specified xylan yield (defined as $100\% - X^*$) and plotting vs β. This plot for uncatalyzed kinetics and two different initial temperatures is presented in Fig. 8.

A third type of plot can be prepared that only considers the error between the isothermal and transient profiles at an instantaneous time by using the %*ID* and plotting the same parameters shown in Fig. 8. Figure 9 shows this plot for the uncatalyzed model.

Discussion

The dimensionless rate constant that was developed in the present work is directly related to the tube radius squared and the kinetic rate constant assuming first-order kinetics for xylan hydrolysis and inversely related to the thermal diffusivity of the contents of the tube. Therefore, it can be viewed as a ratio of the reaction rate (k) to the rate of heat conduction (R^2/α for a tube), and the larger the value of β, the larger the expected deviation from isothermal operation. This dimensionless group was used to determine the relative effect of variation of the variables that comprise it (radius, kinetic constants, reaction temperature, and thermal diffusivity of tube contents). However, to establish the validity of this dimensionless

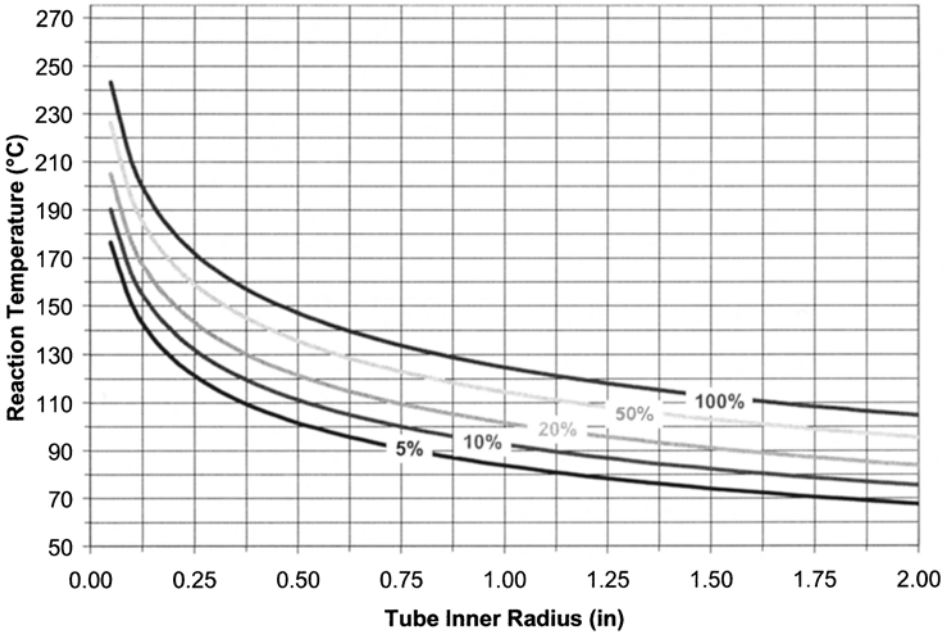

Fig. 6. %*AD* as function of tube inner radius and reaction temperature for catalyzed model, initial temperature of 20°C, and 0.5 wt% acid concentration.

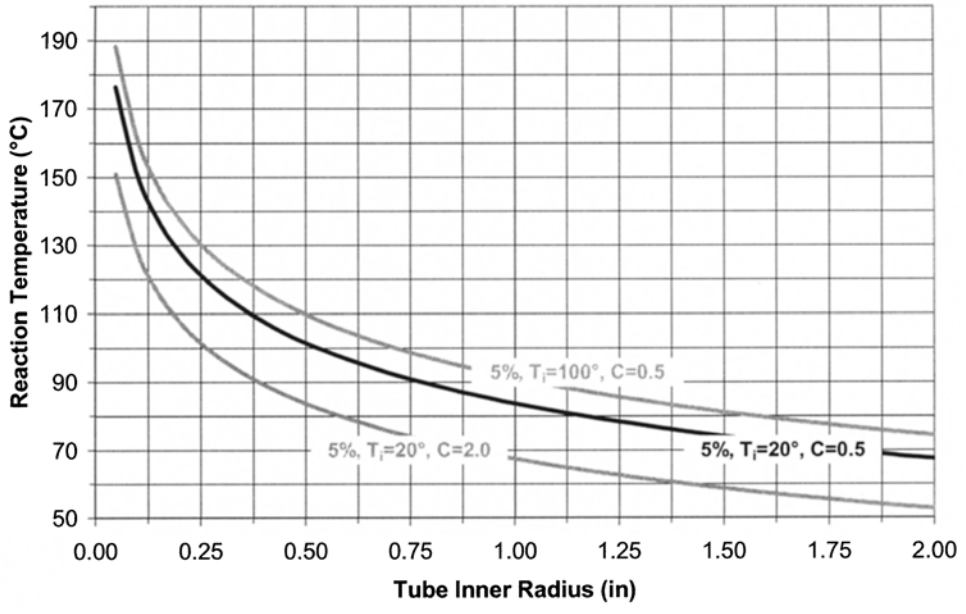

Fig. 7. %*AD* as function of tube inner radius and reaction temperature for catalyzed model, initial temperature of 20 and 100°C, and 0.5 and 2.0 wt% acid concentration with each line representing the limit for an error of 5%.

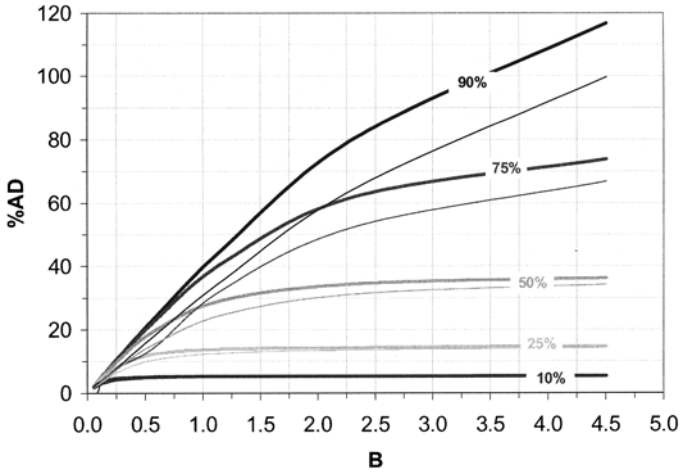

Fig. 8. Percentage xylan yield as function of %*AD* and β for uncatalyzed model and initial temperatures of 20°C (thick solid lines) and 100°C (thin solid lines).

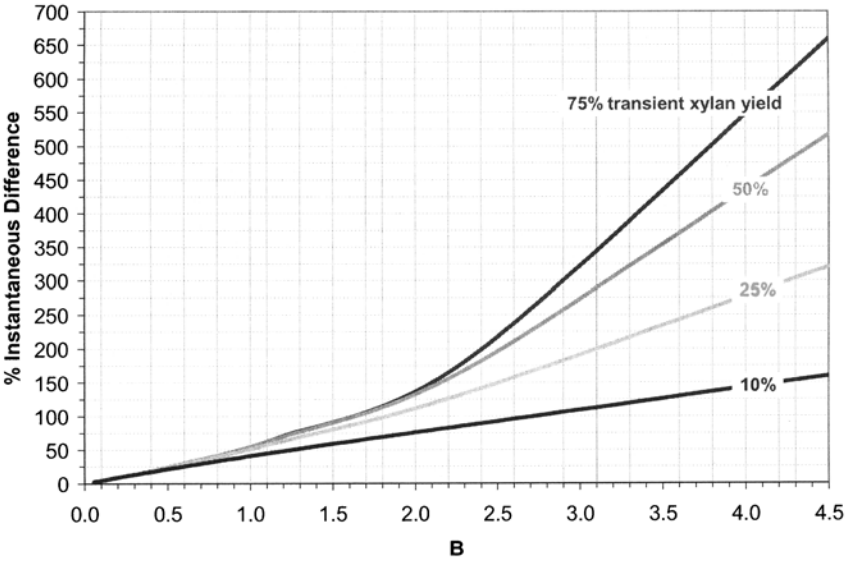

Fig. 9. Percentage xylan yield as a function of %*ID* and β for uncatalyzed model and initial temperature of 20°C.

constant, a relationship between β and quantitative measures of deviation must be shown. The Excel model and Figs. 3–9 described in the previous section successfully established that three quantitative parameters of deviation from isothermal operation could be related to the dimensionless rate constant, β, for both acid-catalyzed and uncatalyzed kinetic models. A quantitative indicator of the difference between the isothermal and transient xylan profiles generated for specific kinetic parameters can be directly

calculated by using plots such as in Figs. 3 and 4. For example, to calculate the deviation for 1/2-in. OD tubes and 0.5 wt% acid, heated from room temperature to a reaction temperature of 160°C, β would first be calculated using Eq. 15. After inserting the terms in appropriate units, the resulting value of β is 1.24, and, therefore, from Figs. 3B and 4B, the SS_E and %*AD* can be found to be approximately 22 and 40%, respectively. Figures 5–7 incorporate the linear relationships from Fig. 4 to eliminate the intermediate step of calculating β. For this example, using Fig. 6 with a 1/2-in. OD tube (0.21-in. inner radius) and 160°C gives an area difference of <50%.

From the two methods that were used to calculate a quantitative deviation based on the time history of the xylan profile, the %*AD* is the most useful because it gives a relative area so it does have some physical meaning and has a linear relationship with β over a much larger range of values. The %*AD* parameter also provides a basis for comparison of different kinetic studies that have been previously reported in the literature and for determining when assumptions of isothermal operation appear valid. The third quantitative parameter, %*ID*, is useful as a means to estimate the error in any data point.

It is important to note that this analysis is inherently dependent on assumptions in both the heat transfer and kinetic model that may not always be valid. For example, the heat transfer model assumes that heat transfer in the tubular batch reactors is controlled by conduction and that convection forces are not important. Although experimental measurements of centerline temperatures in tubular reactors loaded with low (5%) to high (100%) solids concentrations follow the model prediction, there may be situations in which convection forces may impact and speed up heat transfer in tubular batch reactors. Additionally, the kinetic models are based on first-order kinetics although many researchers have found biphasic kinetics to best fit their data. For these reasons, the results of this analysis should be viewed in relative rather than absolute terms and utilized primarily as a tool to guide tubular reactor analysis and design and interpret the accuracy of the results.

Conclusions

The results of this analysis indicate that it is very important to validate the assumption of isothermal operation for both acid-catalyzed and uncatalyzed hydrolysis in batch reactor tubes. A dimensionless rate constant consisting of the ratio of the reaction rate to the heat conduction rate was shown to be useful as a tool to quantitatively determine the range of experimental conditions in which the isothermal assumption is reasonable and those in which this assumption is questionable. Increasing factors that speed up the reaction rate, such as reaction temperature and acid concentration, were shown to increase the dimensionless rate constant and lead to larger errors, while increasing factors that speed up the heat conduction rate, such as thermal diffusivity or smaller reactor tubes, were shown to decrease the dimensionless rate constant and the resulting error.

An Excel spreadsheet model was created to calculate the traditional isothermal xylan profile as well as a transient xylan profile based on the transient temperature profile in the reactor that is expected if conduction is controlling. Three quantitative measures were developed to describe the differences between these profiles and were shown to be directly related to the dimensionless rate constant. Through the use of reactor design curves, it was demonstrated that experimental studies that utilize tubular reactors larger than 1/2-in. are dramatically affected by temperature transients in all but the slowest reaction rate conditions (e.g., low temperatures without addition of acid). Furthermore, our results indicate that if the model assumptions are valid, deviation from isothermal operation is expected to be significant in many published experimental studies.

Future work on this project will include the utilization of a wider variety of kinetic data sets, as well as our own laboratory data, to determine whether there is a universal relationship between the dimensionless constant and the deviation from isothermal operation. It will also be important to determine how temperature transients affect further reaction products such as oligomers, monomers, and degradation products as well as to conduct experimental work to verify model predictions of the effects of temperature transients.

Acknowledgments

This research was made possible through the support of the USDA National Research Initiative Competitive Grants Program (contract 2001-35504-10041) and the Thayer School of Engineering at Dartmouth College.

References

1. Montane, D., Salvado, J., Farriol, X., and Chornet, E. (1993), *Biomass Bioeng.* **4–6,** 427–437.
2. Torget, R. W., Kim, J. S., and Lee, Y. Y. (2000), *Ind. Eng. Chem. Res.* **39,** 2817–2825.
3. Baugh, K. D. and McCarty, P. L. (1988), *Biotechnol. Bioeng.* **31,** 50–61.
4. Chen, R., Lee, Y. Y., and Torget, R. (1996), *Appl. Biochem. Biotechnol.* **57/58,** 133–146.
5. Tillman, L. M., Abaseed, A. E., Lee, Y. Y., and Torget, R. (1989), *Appl. Biochem. Biotechnol.* **20/21,** 107–117.
6. Jacobsen, S.E. (2000), MS thesis, Thayer School of Engineering, Dartmouth College, Hanover, NH.
7. Jacobsen, S. E. and Wyman, C. E. (2001), *Appl. Biochem. Biotechnol.* **91-93,** 377–386.
8. Bird, R. B., Stewart, W. E., and Lightfoot, E. N. (1960), *Transport Phenomena*, John Wiley, New York, NY.
9. Garrote, G., Dominguez, H., and Parajo, J. C. (2001), *Process Biochem.* **36,** 571–578.